NeuroImage: Clinical 35 (2022) 103140

Contents lists available at ScienceDirect

NeuroImage: Clinical

journal homepage: www.elsevier.com/locate/ynicl

Involvement of cerebellar and subcortical connector hubs in schizophrenia

Maeri Yamamoto [a,1], Epifanio Bagarinao [b,c,1], Masanori Shimamoto [a], Tetsuya Iidaka [b,*], Norio Ozaki [a]

[a] Department of Psychiatry, Nagoya University, Graduate School of Medicine, Nagoya, Aichi, Japan
[b] Brain & Mind Research Center, Nagoya University, Nagoya, Aichi, Japan
[c] Department of Integrated Health Sciences, Nagoya University Graduate School of Medicine, Nagoya, Aichi, Japan

ARTICLE INFO

Keywords:
Connector hub
Schizophrenia
Network analysis
Thalamus
Basal ganglia
Biomarker

ABSTRACT

Background: Schizophrenia is considered a brain connectivity disorder in which functional integration within the brain fails. Central to the brain's integrative function are connector hubs, brain regions characterized by strong connections with multiple networks. Given their critical role in functional integration, we hypothesized that connector hubs, including those located in the cerebellum and subcortical regions, are severely impaired in patients with schizophrenia.

Methods: We identified brain voxels with significant connectivity alterations in patients with schizophrenia (n = 76; men = 43) compared to healthy controls (n = 80; men = 43) across multiple large-scale resting state networks (RSNs) using a network metric called functional connectivity overlap ratio (FCOR). From these voxels, candidate connector hubs were identified and verified using seed-based connectivity analysis.

Results: We found that most networks exhibited connectivity alterations in the patient group. Specifically, connectivity with the basal ganglia and high visual networks was severely affected over widespread brain areas in patients, affecting subcortical and cerebellar regions and the regions involved in visual and sensorimotor processing. Furthermore, we identified critical connector hubs in the cerebellum, midbrain, thalamus, insula, and calcarine with connectivity to multiple RSNs affected in the patients. FCOR values of these regions were also associated with clinical data and could classify patient and control groups with > 80 % accuracy.

Conclusions: These findings highlight the critical role of connector hubs, particularly those in the cerebellum and subcortical regions, in the pathophysiology of schizophrenia and the potential role of FCOR as a clinical biomarker for the disorder.

1. Introduction

Schizophrenia is a severe psychiatric disorder characterized by delusions, hallucinations, social withdrawal, impaired motivation, and cognitive dysfunction (Owen et al., 2016). Although schizophrenia's pathophysiology remains unclear, it has been widely regarded as a neurodevelopmental disorder of brain connectivity (Bullmore et al., 1997; Friston, 1998). The dysconnection hypothesis, proposed by Friston and colleagues (Friston et al., 2016; Friston, 1998), described schizophrenia as a failure of functional integration within the brain and suggested that the disorder's pathophysiology is a result of abnormal connections. The cerebellum and subcortical structures such as the thalamus and basal ganglia have been thought to play an important role in the pathogenesis of schizophrenia (Andreasen et al., 1998; Andreasen

Abbreviations: aSal, anterior salience network; Aud, auditory network; BG, basal ganglia network; CDT, a cluster-defining threshold; CPZ, chlorpromazine; dDMN, dorsal default mode network; FA, flip angle; FC, functional connectivity; FCOR, functional connectivity overlap ratio; FDR, false discovery rate; fMRI, functional magnetic resonance imaging; FOV, field of view; FWEc, family-wise error correction at the cluster level; hVis, high visual network; JART, Japanese version of the National Adult Reading Test; Lang, language network; LECN, left executive control network; PANSS, Positive and Negative Syndrome Scale; PC, principal component; Prec, precuneus network; pSal, posterior salience network; pVis, primary visual network; RECN, right executive control network; ROI, region-of-interest; RSN, resting state network; SMN, sensorimotor network; SVM, support vector machine; TE, echo time; T1w, T1-weighted; TR, repetition time; vDMN, ventral default mode network; Visu, visuospatial network.

* Corresponding author at: Brain & Mind Research Center, Nagoya University, Nagoya, Aichi, Japan.
E-mail address: iidaka@met.nagoya-u.ac.jp (T. Iidaka).

[1] MY and EB contributed equally to this work.

https://doi.org/10.1016/j.nicl.2022.103140
Received 4 March 2022; Received in revised form 29 July 2022; Accepted 30 July 2022
Available online 4 August 2022

and Pierson, 2008; Koshiyama et al., 2018a; Koshiyama et al., 2018b; Okada et al., 2016; Okada et al., 2018; Sasabayashi et al., 2020). Dysconnectivity in the cortical-striatal-thalamic and cortical-cerebellar-thalamic cortical circuits has been reported to be associated with cognitive dysfunction and various symptoms, including psychosis, in patients with schizophrenia (Dandash et al., 2014; Duan et al., 2015; Fornito et al., 2013; Giraldo-Chica and Woodward, 2017; Martino et al., 2018; Yamamoto et al., 2018). These findings suggest that the dysconnection of specific brain circuits might contribute to the pathology of schizophrenia.

Recent advances in neuroimaging techniques have made it possible to investigate the brain's integrative functions by mapping the complex regional interactions comprising whole-brain connectivity. Resting-state functional magnetic resonance imaging (fMRI), for instance, has been instrumental in probing the brain's functional architecture, leading to the identification of several large-scale, functional, resting state networks (RSNs) (Beckmann et al., 2005; Biswal et al., 1995; Greicius et al., 2003; Seeley et al., 2007). Furthermore, several studies have demonstrated the significance of these RSNs; their disruptions are associated with psychiatric (Greicius, 2008; Menon, 2011) and neurodegenerative disorders (Dai et al., 2015; Greicius et al., 2004; Kawabata et al., 2018; Yokoi et al., 2018; Yoneyama et al., 2018).

Network analysis using resting-state fMRI also revealed the presence of connector hubs (van den Heuvel and Sporns, 2013), brain areas that have numerous strong interconnections with other regions located within and between RSNs. Given their high degree of connectivity, connector hubs are considered pivotal in coordinating information flow between neural systems, and are crucial for integrating functionally specialized systems (Sporns et al., 2007). Dysfunction of connector hubs has been associated with behavioral and cognitive impairments in several neurological and psychiatric disorders (Buckner et al., 2009; Dai et al., 2015; van den Heuvel and Sporns, 2013), including schizophrenia (Alexander-Bloch et al., 2013; Liu et al., 2008; Lynall et al., 2010; van den Heuvel et al., 2013; Wang et al., 2010). It has also been hypothesized that diminished functioning of key brain hubs in schizophrenia may lead to inefficient information integration between different brain regions (van den Heuvel and Kahn, 2011). Given its critical role in the brain's integrative functions, we hypothesized that the connectivity of connector hubs, including those in the cerebellum and subcortical regions, is significantly impaired in patients with schizophrenia compared to controls.

A commonly used network metric to identify connector hubs is the participation coefficient (Guimera and Nunes Amaral, 2005; Rubinov and Sporns, 2010). In graph theory, this metric quantifies a node's connections to the different communities in the network. The more evenly the node is connected to these communities, the higher its participation coefficient. On the other hand, if the node's connections are mainly restricted to within its community, its participation coefficient is 0. To estimate this metric for the whole-brain network at the voxel-level resolution entails huge memory footprint and computing requirement. Thus, existing approaches typically employ brain parcellation to reduce the number of nodes to a few hundreds. Consequently, identified connector hubs are very limited in spatial resolution and could vary with the parcellation method used. Often, critical subcortical and cerebellar regions are also excluded as most parcellation methods are mainly based on the cerebral cortex. Moreover, this metric only quantifies whole-brain connections rather than connections with specific RSNs; hence changes in the metric cannot be readily associated with any specific RSN.

In this study, we examined changes in the whole-brain connectivity in patients with schizophrenia using a network metric called functional connectivity overlap ratio (FCOR) (Bagarinao et al., 2020). By quantifying a voxel's connections to specific RSNs, FCOR can be used to identify regions with high between-network connectivity at the voxel level, enabling the identification of connector hubs across the whole brain (Bagarinao et al., 2020), including the cerebellum (Kawabata et al., 2022) and other subcortical regions (Kawabata et al., 2021). Using resting-state fMRI data, FCOR maps for several well-known RSNs were generated and used to examine and compare connectivity changes across the whole brain between patients with schizophrenia and control groups. Affected connector hubs were identified by examining regions with significant connectivity alterations to multiple RSNs. Moreover, we examined the predictive power of FCOR values in the affected hub regions to distinguish between patients and controls using linear support vector machines (SVMs).

2. Methods and materials

2.1. Study participants

Seventy-six patients with schizophrenia and 80 healthy controls participated in the study. Table 1 presents the demographic and clinical data of the participants. The patients were recruited from Nagoya University Hospital and its affiliated hospitals and were diagnosed based on the Diagnostic and Statistical Manual of Mental Disorders, 4th Edition diagnostic criteria (American Psychiatric Association, 2000) using a structured interview. The patients were excluded if they had a history of DSM-IV axis I psychiatric disease other than schizophrenia. Current clinical symptom severity was assessed using the Positive and Negative Syndrome Scale (PANSS) (Kay et al., 1987). The dose of antipsychotic medication received at the time of scanning was evaluated using chlorpromazine (CPZ) equivalents (Inada and Inagaki, 2015). The healthy controls had no history of psychiatric or neurological disorders (based on the Structured Clinical Interview for Diagnosis, non-patient version) (First et al., 2002) and did not use any psychoactive medications. Intelligence quotient scores were estimated using the Japanese version of the National Adult Reading Test (JART) (Matsuoka et al., 2006). Handedness was assessed using the Edinburgh Handedness Inventory (Oldfield, 1971). All study procedures were carried out in accordance with the Declaration of Helsinki and approved by the Nagoya University Graduate School of Medicine and Nagoya University Hospital Ethics Review Committee. All participants provided written informed consent before joining the study.

Table 1
Demographic and clinical data of the participants.

Variable	Schizophrenia (n = 76)	Controls (n = 80)	Statistics
Age (years)	42.7 (10.2)	40.8 (9.6)	$t(154) = -1.19$, $p = 0.24$
Sex (male/female)	43/33	43/37	$\chi^2 = 0.13$, $p = 0.72$
Handedness (right/left/both)	64/3/5	73/2/5	
Education[a]	13.4 (2.7)	16.3 (1.6)	$t(146) = 7.99$, $p = 3.83 \times 10^{-13}$
Estimated IQ (JART) [b]	98.0 (10.9)	107.6 (7.2)	$t(144) = 6.37$, $p = 2.34 \times 10^{-9}$
Age at onset	24.1 (6.7)		
Duration of illness (years)	18.5 (11.3)		
Medication (CPZ equivalent) (mg) [c]	564.6 (373.1)		
PANSS Total[d]	66.1 (22.4)		
PANSS Positive[d]	15.4 (6.1)		
PANSS Negative[d]	16.9 (6.6)		

Data are mean (standard deviation).
Note: IQ, Intelligence quotient; JART, Japanese version of the National Adult Reading Test; CPZ, chlorpromazine; PANSS, Positive and Negative Syndrome Scale.
[a] Information is missing for 5 patients and 3 controls.
[b] Information is missing for 10 patients.
[c] Information is missing for 7 patients.
[d] Information is missing for 12 patients.

2.2. MRI data

All participants were scanned at the Brain & Mind Research Center, Nagoya University, using a Siemens Magnetom Verio 3.0 T MRI scanner with a 32-channel head coil (Siemens, Erlangen, Germany). For each participant, high-resolution T1-weighted (T1w) MRI and resting-state fMRI data were obtained. The T1w images were acquired using a three-dimensional magnetization prepared rapid acquisition gradient echo (MPRAGE, Siemens, Erlangen, Germany) sequence (Mugler and Brookeman, 1990) with the following imaging parameters: repetition time (TR) = 2500 ms, echo time (TE) = 2.48 ms, inversion time = 900 ms, flip angle (FA) = 8 degrees, field of view (FOV) = 256, 256 × 256 matrix dimension, 192 sagittal slices with 1-mm thickness, in-plane voxel resolution of 1.0 × 1.0 mm^2, and total scan time of 5 min and 49 s. For the resting-state fMRI data, an ascending gradient-echo echo-planar imaging sequence was used, with the following parameters: TR = 2.5 s, TE = 30 ms, FOV = 192 mm, 64 × 64 matrix dimension, 39 transverse slices with a 0.5 mm inter-slice interval and 3-mm thickness, FA = 80 degrees, and total scan time of 8 min and 15 s. All participants were instructed to close their eyes but stay awake during the scan.

2.3. Image preprocessing

All images were preprocessed using Statistical Parametric Mapping (SPM12, Wellcome Trust Center for Neuroimaging, London, UK) running on MATLAB (R2020a, MathWorks, Natick, Massachusetts, USA). The preprocessing pipeline is detailed in our previous paper (Bagarinao et al., 2020). Briefly, T1w images were segmented using SPM12′s segmentation approach (Ashburner and Friston, 2005) to extract bias-corrected T1w images and transformation information from subject space to the Montreal Neurological Institute (MNI) template space. After removing the first 5 volumes, the resting-state fMRI data, were slice-time corrected, realigned, co-registered to the bias-corrected T1w image, normalized to the MNI template space using the obtained transformation information, resampled to 3.0 × 3.0 × 3.0 mm^3 voxel resolution, and smoothed using a 6-mm full-width-at-half-maximum three-dimensional Gaussian filter. Effects of head motion were regressed out using 24 motion-related regressors that included the six estimated motion parameters (three parameters each for translation and rotation), their derivatives, and the squares of the original estimates and their derivatives. Head motion, quantified using mean frame-wise displacement estimated from motion parameters (Power et al., 2014), did not significantly differ (non-parametric rank sum test $p = 0.2756$) between patients and controls. In addition, signals from the white matter and cerebrospinal fluid, the global signal, and their derivatives were also regressed. Finally, a bandpass filter (0.01 to 0.1 Hz) was applied.

2.4. FCOR estimation

FCOR maps associated with several well-known RSNs were computed using the preprocessed resting-state fMRI data. FCOR quantifies the spatial extent of a voxel's connection to a given large-scale RSN and can be used to identify connector hubs by examining voxels with significant connections to multiple RSNs. The approach for constructing FCOR maps is described in our previous paper (Bagarinao et al., 2020). Briefly, we performed a whole-brain, seed-based connectivity analysis for each voxel and generated the voxel's functional connectivity (FC) map. The voxel's FCOR value was estimated as the spatial extent (number of voxels) of the overlap between the constructed FC map and a reference RSN template divided by the number of voxels comprising the RSN template. FCOR values could range from "0″ for no overlap to "1" when the RSN template is entirely within the voxel's FC map. An increase in the FCOR value indicates an increase in the number of connections to a given RSN, whereas a decrease indicates the opposite. A whole-brain FCOR map for a given reference RSN can be generated by repeating the same process for all voxels within the brain. Finally, the FCOR map was standardized by converting FCOR values into z-scores so that the maps could be averaged and compared across participants (Buckner et al., 2009).

2.5. Statistical analysis of FCOR maps

Following our previous study (Bagarinao et al., 2020), we used Shirer's 14 RSN templates, identified using independent component analysis (Shirer et al., 2012), as reference RSNs. The templates included the dorsal default mode network (dDMN), ventral default mode network (vDMN), precuneus network (Prec), anterior salience network (aSal), posterior salience network (pSal), left executive control network (LECN), right executive control network (RECN), visuospatial (dorsal attention) network (Visu), language network (Lang), basal ganglia network (BG), primary visual network (pVis), high visual network (hVis), sensorimotor network (SMN), and auditory network (Aud). For each participant, we generated 14 whole-brain standardized FCOR maps, one for each RSN. Then, we compared the maps obtained from healthy controls and patients with schizophrenia using a general linear model with independent variables representing the control group (equal to "1″ when participant belong to the control group and "0" otherwise), patient group (equal to "1" when participant belong to the patient group and "0" otherwise), age, sex, and mean frame-wise displacement. To identify regions with significant difference in FCOR values, two contrast maps were generated; namely, controls > patients and controls < patients. In addition, two contrast maps representing significant mean FCOR values for controls and patients were also generated. The striatum, main component of BG, is the primary target of all antipsychotics (Hall et al., 1994) and increased functional connectivity of the striatum by antipsychotic treatment has been reported (Sarpal et al., 2015). To examine the effect of antipsychotics in FCOR values in the patient group, we also performed a separate regression analysis using CPZ values as regressor of the FCOR maps of the BG from the patient group. The threshold for the resulting statistical maps was set at $p < 0.05$, corrected for multiple comparisons using a family-wise error correction at the cluster level (FWEc) with a cluster-defining threshold (CDT) set at $p = 0.001$. We used SPM12 for all whole-brain statistical analyses.

2.6. Identification of connector hubs

We performed conjunction analysis using the final statistical maps of the 14 RSNs. Voxels were assigned a value of "1″ or "0" depending on whether they met the statistical threshold or not, respectively. The binarized statistical maps of the 14 RSNs were then combined to generate the conjunction map. To identify regions with significantly altered connectivity to several RSNs, two conjunction maps were constructed, one for each contrast (controls > patients and controls < patients). In these maps, each voxel's value represented the number of RSNs where the given voxel showed significant connectivity alterations in the patient group. From the constructed conjunction maps, candidate affected connector hubs were identified from the local peaks with values above three. Regions-of-interest (ROIs) from contiguous voxels with peak values were then constructed. To validate that the constructed ROIs were indeed connector hubs, we performed seed-based connectivity analyses with the ROIs as seed regions using the preprocessed resting-state fMRI data from healthy controls. A group level connectivity map for each ROI was constructed using a one-sample *t*-test of individual connectivity maps. Significant connections were identified by thresholding the resulting statistical map with an FWEc $p < 0.05$ and CDT $p = 0.001$. FCOR values were estimated using the group-level connectivity map of each ROI. We also identified the locations of potential connector hubs in patient and control groups separately. For this, two conjunction maps were constructed using the contrast maps extracting significant mean FCOR values for each group. In these conjunction maps, each voxel's value represents the number of RSNs where the voxel has significant connections. Voxels with significant connections with multiple

RSNs represent potential connector hubs.

2.7. Connector-hub-level analyses using FCOR features

Finally, we computed the mean FCOR value within the constructed ROIs (connector hubs) for each RSN to further examine the significance of the identified connector hubs. Each connector hub is therefore represented by 14 mean FCOR values. First, we examined the predictive power of FCOR values in altered connector hubs by using them as features to distinguish patients from healthy controls. Linear SVMs, with the regularization parameter set to the default value of "1" were used for this classification problem. We used a MATLAB version of LIBSVM (Chang and Lin, 2011) to perform tenfold cross-validation to evaluate the SVMs' performance. Next, we examined any association of FCOR values with the patients' clinical characteristics. Only FCOR values of the identified connector hubs from the patient group were used in this analysis. Given the large number of features (number of identified connector hubs × 14 RSNs) involved, we undertook dimensionality reduction using principal component analysis and included only the top principal components (PCs) that cumulatively accounted for >50 % of the FCOR variance in the patient group. The association between component scores and clinical data, which included age, disease duration, CPZ equivalents, JART total IQ, PANSS total, negative, and positive scores, was estimated using Spearman's correlation.

3. Results

3.1. Widespread FCOR alterations in schizophrenia

We observed widespread alterations of FCOR values associated with all RSNs in the patient group compared to the healthy controls (Fig. 1, Supplementary Figure S1). The BG showed the highest number of voxels with significant FCOR reductions, followed by the hVis, RECN, aSal, and vDMN (Fig. 1a). Intriguingly, the number of voxels exhibiting significantly higher FCOR values associated with the BG and hVis in the patient group was higher than the number of voxels with significantly lower FCOR values. FCOR values associated with the LECN showed the least alterations, followed by those associated with the Lang. Contrast maps for the four RSNs with the highest number of affected voxels are shown in Fig. 1(b–e) and for the rest of the RSNs in Supplementary Figure S1. Significant clusters, including peak locations in MNI coordinates and sizes, are summarized in Table 2 and Supplementary Table S1.

We observed the following in the patient group compared to the controls: (1) significantly lower BG-associated FCOR values in the cerebellum, midbrain, thalamus, and mid/anterior cingulate gyrus, and clusters in bilateral supramarginal gyrus, right superior frontal gyrus, and left middle frontal gyrus (Fig. 1b, Table 2); (2) higher FCOR values in the primary-processing-associated regions such as the visual, sensorimotor, and subcortical regions (including caudate and putamen); (3) the BG's connectivity was significantly lower with the subcortical areas and cerebellum, and significantly higher with the visual and sensorimotor processing areas; (4) similar changes were observed in the RECN (Fig. 1d): FCOR values were significantly lower in the subcortical areas and the cerebellum, and higher in cortical areas, including the superior frontal gyrus, orbital gyrus, postcentral gyrus, precentral gyrus, superior occipital gyrus, and occipital pole; (5) FCOR values associated with the hVis (Fig. 1c) were significantly lower in the bilateral occipital fusiform gyrus, middle occipital gyrus, superior parietal lobule, left precentral gyrus, and middle frontal gyrus, and significantly higher in the cerebellum, other subcortical areas, right superior frontal gyrus, and right

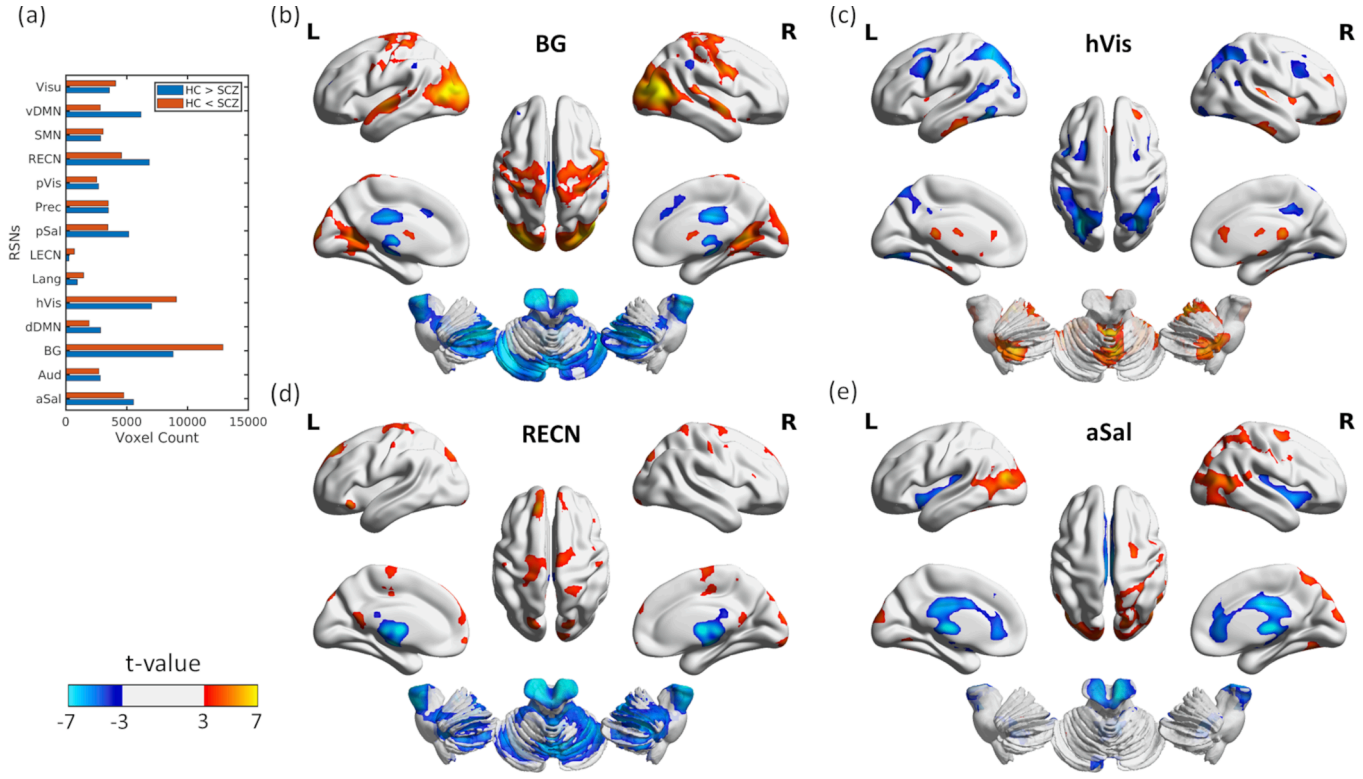

Fig. 1. Regions showing significant (family-wise error correction at the cluster level, $p < 0.05$; cluster-defining threshold, $p = 0.001$) functional connectivity overlap ratio (FCOR) changes in patients with schizophrenia for different resting-state networks (RSNs). (a) Total number of voxels where FCOR values for several RSNs were significantly lower (blue) or higher (red) in the patient group (SCZ) than the healthy control (HC) group. (b)–(e) Contrast maps showing the locations of these voxels for the basal ganglia network (BG), high visual network (hVis), right executive control network (RECN), and anterior salience (aSal) network, respectively. These are the top four networks showing the most regions with significant FCOR changes. Regions shown in red-yellow indicate significantly higher FCOR values in patients (HC < SCZ), while those shown in blue-light blue indicate significantly lower FCOR values in patients than controls (HC > SCZ).

Table 2
Regions showing significant (family-wise error correction at the cluster level, $p < 0.05$; cluster-defining threshold, $p = 0.001$) changes in functional connectivity overlap ratio values associated with the basal ganglia network, high visual network, right executive control network, and anterior salience network.

Contrast	X (mm)	Y (mm)	Z (mm)	z-Value	Cluster Size	Area	Other Peaks
BG							
HC > SCZ	−6	−15	3	7.84	8096	L ThP	L Cer, R Cer
	30	57	24	5.44	249	R SFG	
	63	−42	51	4.91	217	R SMG	
	−66	−45	42	4.46	125	L SMG	
	−33	48	27	3.91	141	L MFG	
HC < SCZ	57	−66	12	7.5	9387	R IOG	L MOG, L IOG
	27	−9	69	6.22	3383	R PrG	R PoG, L PrG
	6	6	6	4.42	148	R Cau	L Pu
hVis							
HC > SCZ	−27	−81	−3	7.5	3177	L OFuG	L MOG, L FuG
	30	−75	−3	6.99	3060	R OFuG	R FuG, R MOG
	−39	3	33	5.41	826	L PrG	L MFG
HC < SCZ	12	6	78	6.88	8960	R SFG	
	63	−57	6	4.65	131	R MTG	R AnG
RECN							
HC > SCZ	9	−9	3	Inf	6878	R ThP	Brainstem, L ThP
HC < SCZ	−15	42	45	5.99	716	L SFG	L FRP
	−42	27	−21	5.76	189	L POrG	
	−63	−6	36	4.89	1493	L PoG	L SFG, R SMC
	60	−9	42	4.78	513	R PoG	R OpIFG, R PrG
	−21	−84	45	4.75	886	L SOG	R SOG, L OCP
	18	−99	−9	4.67	127	R OCP	
	3	−66	12	4.33	350	R Calc	L PCgG, L LiG
	21	−45	69	3.85	139	R SPL	R PCu
	−21	−96	−15	3.82	169	L OFuG	L OCP, L IOG
aSal							
HC > SCZ	−30	9	−9	7.48	4773	L AIns	R ThP, L ThP
	12	−48	−33	5.26	578	R Cer	L Cer
	−6	−81	−27	4.47	214	L Cer	R Cer
HC < SCZ	−42	−78	15	6.1	4762	L MOG	

Abbreviations: BG, basal ganglia network; hVis, high visual network; RECN, right executive control network; aSal, anterior salience network; HC, healthy control group; SCZ, patients with schizophrenia group; ThP, thalamus proper; Cer, cerebellum; SFG, superior frontal gyrus; SMG, supramarginal gyrus; MFG, middle frontal gyrus; IOG, inferior occipital gyrus; MOG, middle occipital gyrus; PrG, precentral gyrus; PoG, postcentral gyrus; Cau, caudate; Pu, putamen; OFuG, occipital fusiform gyrus; FuG, fusiform gyrus; MTG, middle temporal gyrus; AnG, angular gyrus; FRP, frontal pole; POrG, posterior orbital gyrus; SMC, supplementary motor cortex; OpIFG, opercular inferior frontal gyrus; SOG, superior occipital gyrus; OCP, occipital pole; Calc, calcarine; PCgG, posterior cingulate gyrus; LiG, lingual gyrus; SPL, superior parietal lobule; PCu, precuneus; AIns, anterior insula; L, left; R, right.

middle temporal gyrus/angular gyrus; and (6) FCOR values were lower for the aSal in the left anterior insula, bilateral thalamus, and the cerebellum, and higher in a cluster with peak location in the left middle occipital gyrus.

The result of the regression analysis of the FCOR maps of the BG with CPZ values in the patients showed a significant positive correlation (z-value 4.12, cluster size 45) in the medial superior frontal gyrus or the bilateral frontal pole (Fig. 2).

3.2. *Significantly impaired Cerebellar, Thalamic, and other cortical connector hubs in schizophrenia*

Fig. 3 shows conjunction maps summarizing the number of RSNs with significant FCOR alterations in the patient group. The MNI coordinates of the center of gravity of clusters showing significant reduction in FCOR values associated with at least four RSNs and their sizes are summarized in Table 3.

Seed-based connectivity analyses using these clusters as seed regions showed that the identified clusters had strong connections with multiple RSNs in healthy controls, indicating that these clusters are indeed connector hubs. Focusing on subcortical and cerebellar connector hubs corresponding to the top six ROIs listed in Table 3, in Fig. 4, we showed the FCOR values of the group-level connectivity maps to illustrate their connection profiles to the different RSNs in the control group. All six connector hubs were strongly connected with the BG. Cerebellar connector hubs were also connected with executive control (LECN, RECN), default mode (Prec), and primary processing (SMN) networks. On the other hand, thalamic connector hubs were connected with salience (aSal, pSal), executive control (RECN), default mode (Prec, dDMN), and primary processing (SMN) networks.

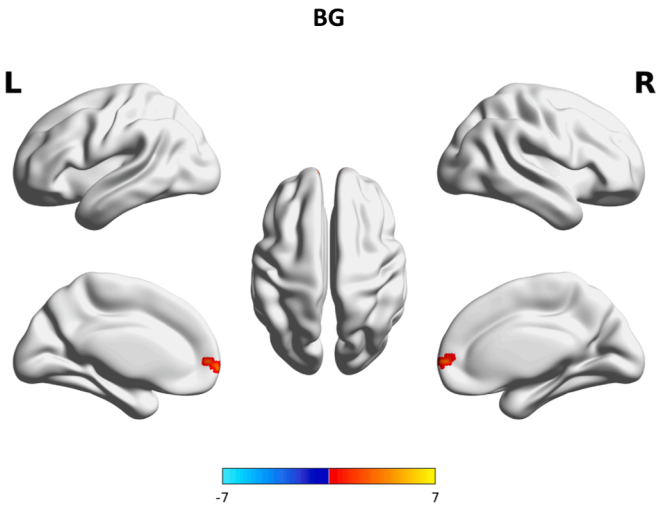

Fig. 2. The whole-brain correlation analysis between the BG-associated FCOR values and the dose of antipsychotics in the patient group. The FCOR values in the medial superior frontal gyrus or the bilateral frontal pole showed a significant positive correlation ($p < 0.05$, corrected for multiple comparisons using family-wise error correction at the cluster level with a cluster-defining threshold set at $p = 0.001$).

Boxplots of the mean FCOR values associated with the 14 RSNs for the identified cerebellar and subcortical connector hubs are also shown

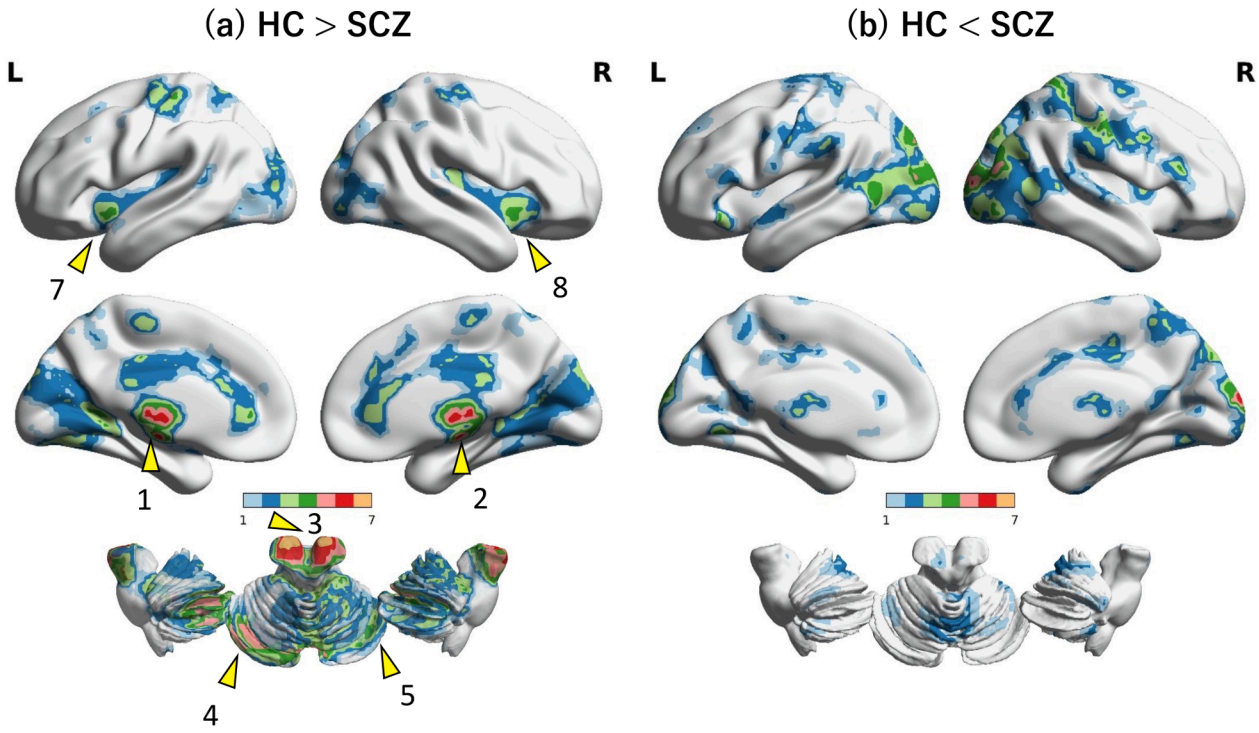

Fig. 3. Conjunction maps for (a) healthy control (HC) > patient group (SCZ) and (b) HC < SCZ contrasts. Voxel values represent the number of resting-state networks (RSNs) where the associated functional connectivity overlap ratio values at the voxel level for the RSNs were significantly altered in the patient group. The yellow arrows and their corresponding numbers indicate the first eight regions of interest listed in Table 3. (Region 6 is not shown in this figure.) (a) The thalamus showed the greatest number of RSNs where its connectivity was significantly lower in the patient group than the control group. This is followed by a region in the midbrain with significantly lower connectivity to seven RSNs, bilateral posterior cerebellum and anterior cerebellum to five RSNs, and bilateral insula and calcarine to four RSNs. Smaller clusters in the postcentral gyrus and anterior cingulate gyrus also showed significantly lower connectivity to four RSNs. (b) In contrast, several clusters (primarily located in the occipital lobe, including the middle occipital gyrus, bilateral cuneus, and left inferior/middle temporal gyrus) showed significantly higher connectivity to at least four RSNs in the patient group than the control group.

Table 3
Identified connector hub regions showing significant reduction in functional connectivity overlap ratio associated with at least four resting-state networks in the patient group compared to the control group.

	Region of Interest	Center of Gravity			Value (Number of RSNs)	Cluster Size (Voxels)
		X (mm)	Y (mm)	Z (mm)		
1	Left Thalamus	−12.20	−11.20	2.76	7	37
2	Right Thalamus	11.50	−10.30	3.63	7	19
3	Midbrain	2.50	−21.80	−13.80	7	18
4	Left Posterior Cerebellum	−33.70	−67.70	−34.30	5	182
5	Right Posterior Cerebellum	9.00	−72.90	−26.90	5	104
6	Anterior Cerebellum	4.47	−48.30	−32.00	5	153
7	Left Insula	−32.70	9.65	−10.50	4	51
8	Right Insula	32.50	12.80	−7.94	4	62
9	Left Calcarine	−18.10	−52.20	4.34	4	29
10	Right Calcarine	26.60	−51.00	5.08	4	39

Abbreviation: RSN, resting-state network.

in Fig. 5. Using a nonparametric rank-sum test, we identified RSNs with significant differences in the mean FCOR values (false discovery rate (FDR) $q < 0.05$) (Supplementary Table S2). The two connector hubs in the thalamus had significantly altered FCOR values for the aSal, BG, dDMN, hVis, LECN, pSal, Prec, pVis, RECN, and SMN in the patients compared to the control group. Furthermore, the patients exhibited significantly lower FCOR values in most networks except in the (primary/high) visual network, where the FCOR values were higher than those in the control group. All six connector hubs that are shown exhibited significantly altered FCOR values for the aSal, BG, hVis, pSal, Prec, and SMN. Moreover, all non-cerebellar connector hubs exhibited alterations in FCOR values for the dDMN.

Separate conjunction maps, which can be used to identify connector hub regions, for the healthy control and patient groups are shown in Supplementary Figure S2. Observed that in the thalamus and several cerebellar regions, the number of RSNs where these regions were strongly connected was significantly reduced in the patient group (Supplementary Figure S2b) as compared to the healthy control group (Supplementary Figure S2a), consistent with Fig. 3.

3.3. Association with clinical data

We also examined the association between FCOR values of the cerebellar and subcortical connector hubs and clinical data. The first three PCs accounted for 59 % of FCOR variance in the patient group. Most clinical data significantly correlated with the second PC score, specifically age ($r = -0.31$, $p = 0.0249$), duration ($r = -0.43$, $p = 0.0008$),

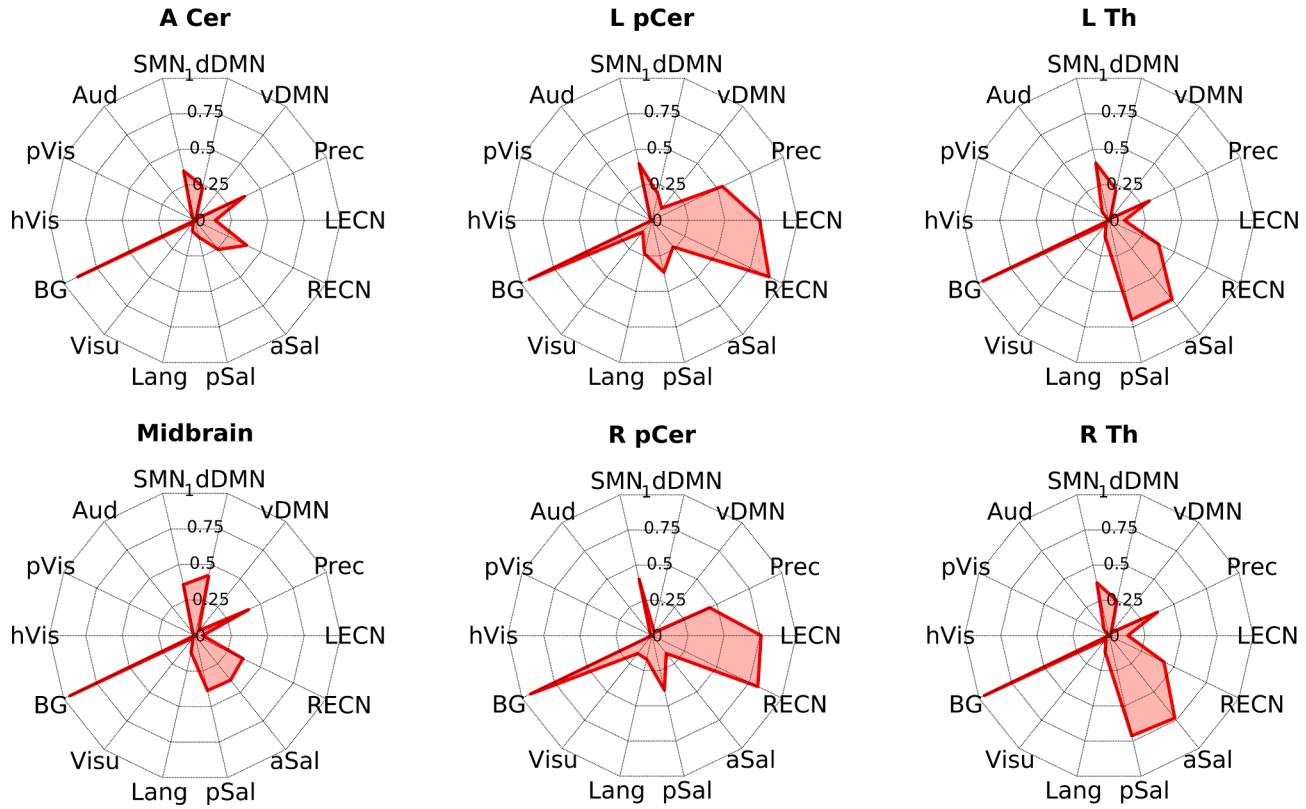

Fig. 4. Functional connectivity overlap ratio (FCOR) values of the identified subcortical and cerebellar connector hubs in healthy controls. Spider plots show that these regions are strongly connected with multiple resting-state networks in healthy controls indicating that they are connector hubs. FCOR values were estimated using a group-level functional connectivity map, obtained using seed-based connectivity analysis, of each connector hub. aSal, anterior salience network; Aud, auditory network; BG, basal ganglia network; dDMN, dorsal default mode network; hVis, high visual network; Lang, language network; LECN, left executive control network; pSal, posterior salience network; Prec, precuneus network; pVis, primary visual network; RECN, right executive control network; SMN, sensorimotor network; vDMN, ventral default mode network; Visu, visuospatial network.

JART total IQ ($r = 0.27$, $p = 0.0390$), and PANSS total ($r = -0.29$, $p = 0.0367$) and PANSS positive ($r = -0.30$, $p = 0.0367$) score (Fig. 6, rightmost column). All p-values were adjusted by FDR correction at $q < 0.05$. We did not observe any association with the first and third PC scores. Weights associated with the first three PCs are plotted in Fig. 6 (first 3 columns). The first PC is mostly associated with the connector hubs' connectivity with the BG as evidenced by the higher coefficient values associated with BG as well as the connectivity between thalamic connector hubs and salience (aSal, pSal) and Aud networks. By contrast, the second PC reflects the associations between cerebellar connector hubs and executive control (LECN, RECN), dDMN, and BG networks, which are positively weighted, as well as between thalamic connector hubs and primary processing (Aud, pVis, hVis) and BG networks, which are negatively weighted. Finally, the third PC is associated with the connections between cerebellar connector hubs and dDMN, hVis, Lang, and LECN as well as between thalamic connector hubs and visual networks (pVis, hVis), which are positively weighted, and between thalamic connector hubs and BG and salience (aSal, pSal) networks, which are negatively weighted.

3.4. High predictive values of FCOR features in affected hub regions

The performance of the classification using the FCOR values of all connector hubs listed in Table 3 was evaluated using a tenfold cross-validation approach (Table 4). Individually, the mean FCOR values of the connector hub located in the left posterior cerebellum showed the highest predictive value (accuracy, 80.77 %), followed by the left thalamus (accuracy, 78.85 %), the right thalamus (accuracy, 78.21 %), and the midbrain (accuracy, 78.21 %). The overall accuracy was 81.41 %.

4. Discussion

Using a novel network measure called FCOR, we found connectivity changes across all large-scale RSNs in patients with schizophrenia compared to healthy controls. Specifically, connections to the BG and hVis over widespread brain regions were significantly altered in patients with schizophrenia. The BG showed significantly lower FCOR values in the subcortical and cerebellar regions but higher FCOR values in the visual and sensorimotor-processing-associated regions. In contrast, the hVis exhibited significantly higher FCOR values in the subcortical and cerebellar regions but lower values in regions associated with higher visual and visuospatial processing. Interestingly, out of the many affected regions, we identified a limited number with significantly altered connections across several RSNs. These regions, located in the cerebellum, midbrain, thalamus, insula, and calcarine have been identified as connector hubs, highlighting the critical role these specialized regions play in the pathophysiology of schizophrenia. To our knowledge, this is the first study to identify connector hub alterations at the voxel-level resolution in the cerebral and subcortical regions in schizophrenia. Finally, FCOR values of the affected hub regions also showed association with clinical data and high predictive values to distinguish patients from controls, signifying their potential as an imaging biomarker to identify patients with schizophrenia.

4.1. Widespread connectivity alterations across several RSNs in patients with schizophrenia

Consistent with existing findings, our results showed that schizophrenia is characterized by widespread connectivity changes involving

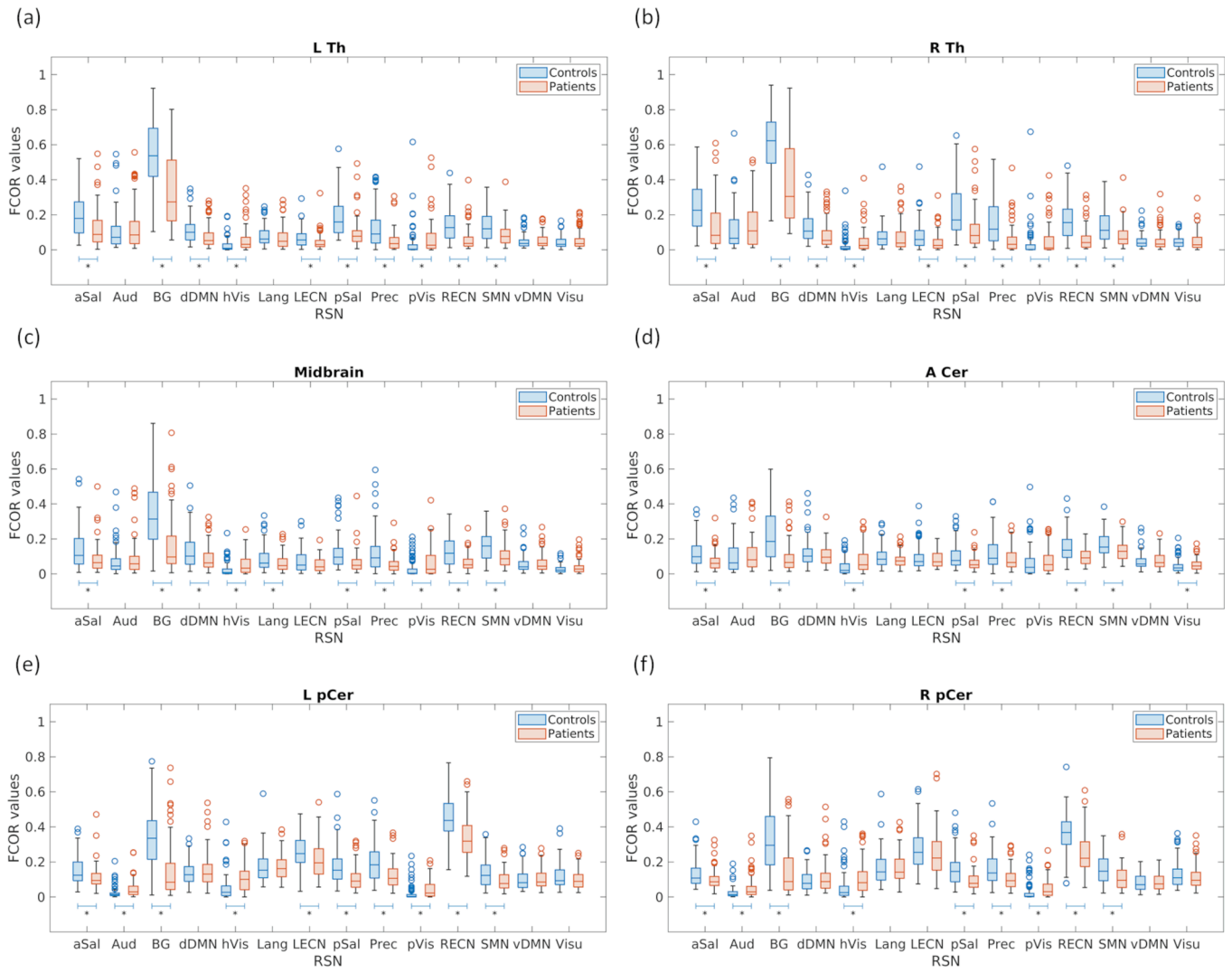

Fig. 5. Boxplots of the mean functional connectivity overlap ratio (FCOR) values associated with the 14 resting-state networks (RSNs) of the identified subcortical and cerebellar connector hubs located in (a) left thalamus (L Th), (b) right thalamus (R Th), (c) midbrain, (d) anterior cerebellum (A Cer), (e) left posterior cerebellum (L pCer), and (f) right posterior cerebellum (R pCer). The pairs indicated by a solid blue line and an asterisk (*) symbol indicate significant differences (false discovery rate, FDR $q < 0.05$) in FCOR values for each RSN between the patient (red) and control groups (blue) using a two-sided rank-sum test. Actual FDR-corrected p-values are listed in the Supplementary Table S2. aSal, anterior salience network; Aud, auditory network; BG, basal ganglia network; dDMN, dorsal default mode network; hVis, high visual network; Lang, language network; LECN, left executive control network; pSal, posterior salience network; Prec, precuneus network; pVis, primary visual network; RECN, right executive control network; SMN, sensorimotor network; vDMN, ventral default mode network; Visu, visuospatial network.

all RSNs, although the degree of these alterations differed. Interestingly, the BG showed the most widespread changes, affecting the subcortical and cerebellar regions as well as regions involved in visual and sensorimotor processing. Since the BG is involved in various brain functions, including motor control, cognition and affective function, its dysfunction could lead to motor deficits, cognitive impairments and psychiatric symptoms at the same time (Macpherson and Hikida, 2019), which is observed in the patients with schizophrenia (Dandash et al., 2014; Duan et al., 2015; Quide et al., 2013; Sui et al., 2015; Zhou et al., 2007). Since the observed alterations in the BG could be affected by the antipsychotics, we performed a whole-brain correlation analysis between the BG-associated FCOR values and the dose of antipsychotics in the patient group and found a significant positive correlation, albeit only in the medial superior frontal gyrus or the bilateral frontal pole. This region did not show up in our analysis comparing patients and controls; therefore, the alterations observed in the BG were not associated with the doses of antipsychotics. However, the precise impact of antipsychotics remains unclear and should be further explored.

The FCOR values associated with the hVis were also severely affected in the patients; higher values were observed in the cerebellar region, whereas lower values were observed in several occipital regions. These findings were consistent with previous studies regarding connectivity alterations (Sendi et al., 2021). The hVis includes the visual association cortex, which is associated with functions including perception and object recognition (Mai, 2012). Alterations in this network could lead to the observed visual-processing impairment in schizophrenia (Javitt, 2009; Kogata and Iidaka, 2018).

4.2. *Connector hub alterations in schizophrenia*

Consistent with our hypothesis, we identified a limited number of connector hub regions in the cerebellum, midbrain, thalamus, insula, and calcarine with significantly altered connections to several RSNs, including the BG, hVis, aSal, and pSal. Greene and colleagues have localized network-specific and multi-network integration zones in the thalamus using precision functional mapping (Greene et al., 2020). Specifically, they identified integration zones in the ventral intermediate thalamus for cingulo-opercular control and somatomotor networks

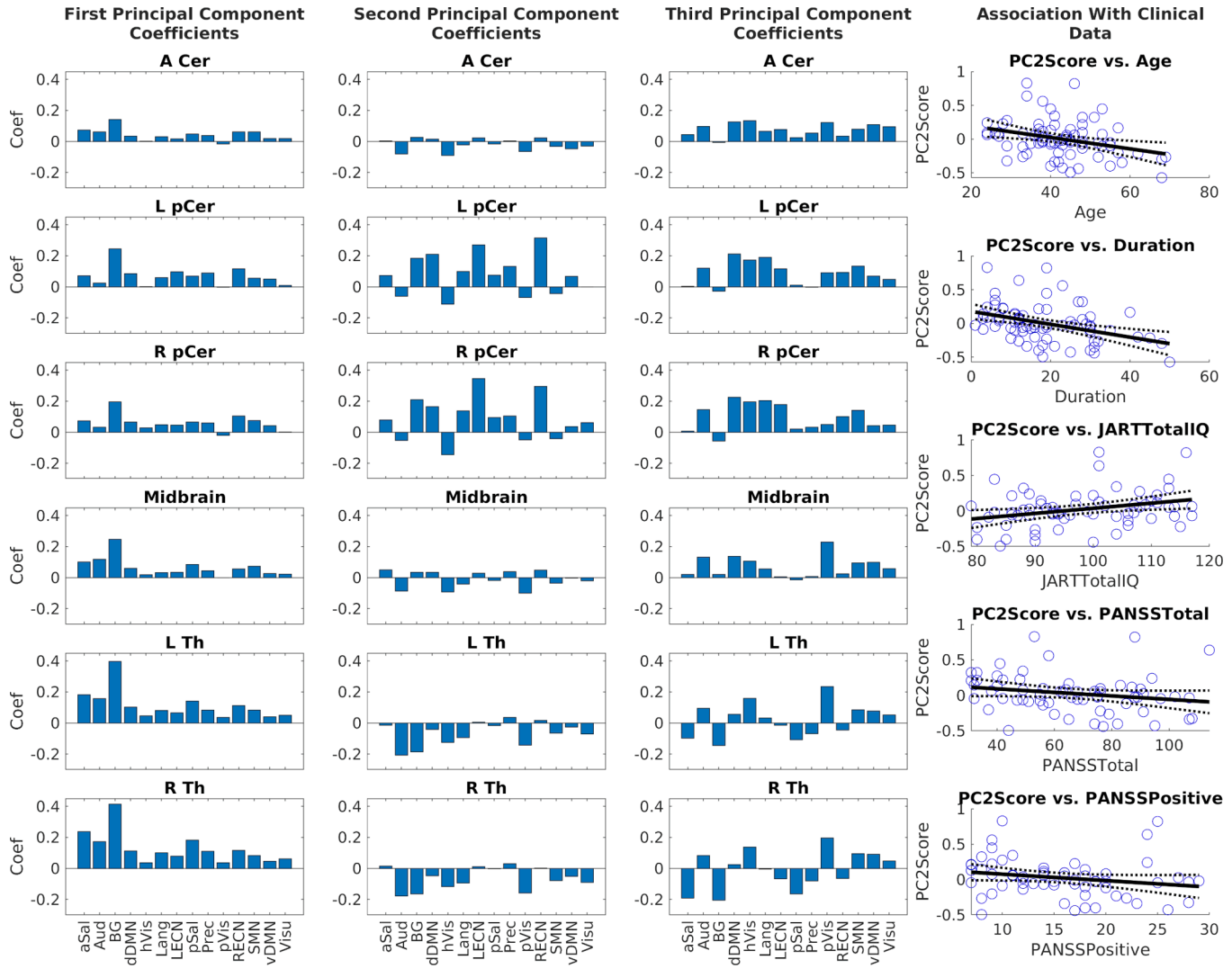

Fig. 6. Principal component analysis of functional connectivity overlap ratio (FCOR) values of subcortical connector hubs. 1st column: Bar plots of the coefficients of the first principal component of the FCOR values of the identified connector hubs in the patient group. In the first component, the connector hubs' FCOR values associated with the basal ganglia network (BG) were weighted higher (more positive), and the midbrain and thalamus connector hubs' FCOR values associated with Sal and auditory networks were also weighted higher. 2nd column: Bar plots of the coefficients of the second principal component. In this component, cerebellar connector hubs' FCOR values associated with BG, default mode (dDMN), and executive control (LECN, RECN) networks were weighted higher, whereas thalamic hubs' FCOR values associated with BG, primary processing (auditory (Aud), high visual (hVis), primary visual areas (pVis), somatosensory (SMN)) and language (Lang) networks were weighted lower (more negative). 3rd column: Bar plots of the coefficients of the third principal component. In this component, cerebellar connector hubs were associated with the dDMN, hVis, Lang, and LECN, while thalamic connector hubs were associated with visual (hVis, pVis), which are positively weighted, and salience (aSal, pSal) and BG, which are negatively weighted. Last column: Association between the second principal component score and clinical data. Circles indicate actual data, solid line represents linear fit, and dotted lines represent confidence.

and the pulvinar for dorsal attention and visual networks. We have also recently identified similar connector hub regions in the anterior insula, thalamus, and cerebellum (Bagarinao et al., 2020; Kawabata et al., 2021). These findings demonstrate the crucial role of connector hubs—located in the cerebral cortex, cerebellum, and subcortical regions—in the pathophysiology of schizophrenia.

Previous studies have also reported hub abnormalities in schizophrenia using resting-state functional MRI (Hummer et al., 2020; Li et al., 2019; Liu et al., 2021; Rubinov and Bullmore, 2013). The main findings of these studies were lower global efficiency and fewer hubs in the cerebellum network (Hummer et al., 2020), reduced nodal efficiency and strength in the hippocampal formation (Li et al., 2019), and a shift in hub locations with more hubs in frontal and occipital regions (Liu et al., 2021) in patients with schizophrenia compared to healthy controls. These different findings may be due to the differences in methodology (such as sample characteristics and analytic methods).

The thalamus plays a significant role in corticocortical communication by controlling information processing, and is involved in sensory and motor systems and cognitive function (Sherman, 2016). Although previous studies have demonstrated reduced prefrontal-thalamic functional connectivity and increased somatosensory-thalamic functional connectivity in patients with schizophrenia (Anticevic et al., 2014; Giraldo-Chica and Woodward, 2017; Yamamoto et al., 2018), our findings specifically implicate the involvement of connector hubs in the thalamus. In addition to those in the thalamus, connector hubs in the cerebellum showed significant alterations in patients with schizophrenia. Because the cerebellum contributes to several RSNs including ECN, Sal and DMN (Habas et al., 2009), the cerebellum is involved in sensorimotor, cognitive, and affective processing (Buckner, 2013; Stoodley and Schmahmann, 2010). Disruption of functional connectivity in the cerebellum in patients with schizophrenia has been reported, particularly in the thalamo-cerebellar and cortico-cerebellar networks

Table 4
Support vector machine classification performance using the mean functional connectivity overlap ratio values associated with the 14 resting-state networks within each region-of-interest as classification features.

Individual ROI	Accuracy (%)	Sensitivity (%)	Specificity (%)	Regional ROI	Accuracy (%)	Sensitivity (%)	Specificity (%)
L Thalamus	78.85	82.89	75.00	**Thalamus**	79.49	78.95	80.00
R Thalamus	78.21	78.95	77.50				
Midbrain	78.21	86.84	70.00				
Anterior Cerebellum	66.03	88.16	45.00	**Cerebellum**	80.77	88.16	73.75
L Posterior Cerebellum	80.77	84.21	77.50				
R Posteror Cerebellum	76.92	86.84	67.50				
L Insula	69.87	86.84	53.75	**Insula**	70.51	82.89	58.75
R Insula	68.59	84.21	53.75				
L Calcarine	72.44	68.42	76.25	**Calcarine**	74.36	76.32	72.50
R Calcarine	76.92	82.89	71.25				

	Accuracy (%)	Sensitivity (%)	Specificity (%)
All ROIs	81.41	84.21	78.75

Abbreviation: ROI, region-of-interest; L, left; R, right.

(Anticevic et al., 2014; Chen et al., 2013; Duan et al., 2015; Wang et al., 2014). Interestingly, FCOR values in cerebellar connector hubs also showed the most predictive power in distinguishing patients with schizophrenia from controls. These findings highlight the vital role cerebellar connector hubs may play in schizophrenia.

FCOR values of the identified connector hubs also showed association with clinical data. Interestingly, the component score of the first PC, contributing the largest variance in FCOR and associated with connections from thalamic connector hubs with the BG, did not show any association with clinical data. By contrast, the second PC's score had associations with multiple clinical data (age, duration of illness, estimated IQ, PANSS total and PANSS positive scores). This may suggest that the first PC is more associated with trait-like connectivity alterations in schizophrenia. Indeed, dysfunction of thalamic connectivity was detected from early stages to chronic patients, and even in high-risk individuals (Giraldo-Chica and Woodward, 2017). The second PC is associated with cerebellar connector hubs' connectivity with the BG, DMN, and ECN, which suggests the importance of the cerebellar connector hubs' connectivity with the core neurocognitive networks (DMN, ECN) in schizophrenia's clinical manifestations. Furthermore, we determined that the second PC's score was associated with PANSS score, consistent with the previous study indicating that cerebellar dysconnectivity was associated with psychotic symptoms in schizophrenia (Brady et al., 2019; Chang et al., 2015).

Overall, our findings suggest that, although connectivity changes across large-scale RSNs involve widespread brain regions, these alterations may be driven by a small number of connector hubs located in the cerebellum, midbrain, thalamus, and cerebral cortex. The BG's influence is also evident considering the significant alterations of FCOR values associated with the BG from these connector hubs (Fig. 5). Neuroimaging studies have shown that the cerebellum, the basal ganglia, and the cerebral cortex form an integrated network, and changes in one node could influence the operation of the other nodes (Bostan and Strick, 2018; Milardi et al., 2019). As connector hubs link several RSNs, impairment of these regions can severely affect the brain's integrative processes, the dysfunction of which could be associated with schizophrenia's diverse symptoms. The relatively high predictive values of FCOR in these connector hubs further support the importance of these critical integrative regions in the pathophysiology of schizophrenia.

5. Limitations

The main limitation of this study is that all patients were on medication at the time of the scan. In addition, we did not assess lifetime cumulative doses of antipsychotic medications. Future studies are needed to examine the effect of antipsychotics on the estimated FCOR values in the medication-naïve patients or off-medication patients. Another limitation is the difficulty in ruling out the potential contribution of head motion during resting-state fMRI scans, which may have induced spurious functional connectivity. Although various methods have been tried to minimize the effects of head motion, no specific method has yet been established (Power et al., 2015). In this study, we regressed out motion-related signals to account for head motion effects and ensured that the amount of head motion did not differ significantly between the patient and control groups. More advanced methods need to be developed to control for head motion in future studies. Finally, differences have been reported in connectivity among brain regions between the eyes-open and eyes-closed states (Jao et al., 2013). The eyes-closed state is associated with a significantly higher variance of the BOLD signal in the visual cortex, somatomotor and somatosensory cortex, auditory cortex, lingual gyrus, fusiform gyrus, parahippocampal gyrus, insula, thalamus, and amygdala, than in the eyes-open state (Jao et al., 2013), some of which were identified as connector hubs in this study. Our findings were obtained using the eyes-closed state, and the eyes-open state was not evaluated.

6. Conclusions

Using a novel network metric called FCOR, we have demonstrated that connector hub regions, including those in the cerebellum, thalamus, and other subcortical regions, are severely impaired in patients with schizophrenia, providing additional evidence to support the dysconnection hypothesis. Furthermore, FCOR features in the affected hub regions exhibited high predictive values (accuracy $>$ 80 %) in distinguishing patients with schizophrenia from healthy controls. These findings highlight the role of connector hubs, particularly in the cerebellum and subcortical regions, in the pathophysiology of schizophrenia and the potential role of FCOR as a clinical biomarker for schizophrenia.

7. Role of the funding source

The study funding sources played no role in study design; in the collection, analysis and interpretation of data; in the writing of the report; and in the decision to submit the article for publication.

CRediT authorship contribution statement

Maeri Yamamoto: Conceptualization, Methodology, Writing – original draft. **Epifanio Bagarinao:** Conceptualization, Methodology, Writing – original draft. **Masanori Shimamoto:** Investigation. **Tetsuya Iidaka:** Writing – review & editing. **Norio Ozaki:** Project administration.

Declaration of Competing Interest

The authors declare that they have no known competing financial interests or personal relationships that could have appeared to influence the work reported in this paper.

Data availability

The authors do not have permission to share data.

Acknowledgements

Funding: This research was supported by AMED [grant numbers JP19dm0207069, JP21wm0425007, JP21dk0307103], and the Japan Society for the Promotion of Science (JSPS) KAKENHI [grant numbers 21H04815, 17K10295, 21K09149, 21K07498].

Appendix A. Supplementary data

Supplementary data to this article can be found online at https://doi.org/10.1016/j.nicl.2022.103140.

References

Alexander-Bloch, A.F., Vertes, P.E., Stidd, R., Lalonde, F., Clasen, L., Rapoport, J., Giedd, J., Bullmore, E.T., Gogtay, N., 2013. The anatomical distance of functional connections predicts brain network topology in health and schizophrenia. Cereb. Cortex 23, 127–138.

Andreasen, N.C., Paradiso, S., O'Leary, D.S., 1998. "Cognitive dysmetria" as an integrative theory of schizophrenia: a dysfunction in cortical-subcortical-cerebellar circuitry? Schizophr. Bull. 24, 203–218.

Andreasen, N.C., Pierson, R., 2008. The role of the cerebellum in schizophrenia. Biol. Psychiatry 64, 81–88.

Anticevic, A., Cole, M.W., Repovs, G., Murray, J.D., Brumbaugh, M.S., Winkler, A.M., Savic, A., Krystal, J.H., Pearlson, G.D., Glahn, D.C., 2014. Characterizing thalamo-cortical disturbances in schizophrenia and bipolar illness. Cereb. Cortex 24, 3116–3130.

Ashburner, J., Friston, K.J., 2005. Unified segmentation. Neuroimage 26, 839–851.

American Psychiatric Association, 2000. Diagnostic and statistical manual of mental disorders: DSM-IV-TR. 4th ed, Washington.

Bagarinao, E., Watanabe, H., Maesawa, S., Mori, D., Hara, K., Kawabata, K., Ohdake, R., Masuda, M., Ogura, A., Kato, T., Koyama, S., Katsuno, M., Wakabayashi, T., Kuzuya, M., Hoshiyama, M., Isoda, H., Naganawa, S., Ozaki, N., Sobue, G., 2020. Identifying the brain's connector hubs at the voxel level using functional connectivity overlap ratio. Neuroimage 222, 117241.

Beckmann, C.F., DeLuca, M., Devlin, J.T., Smith, S.M., 2005. Investigations into resting-state connectivity using independent component analysis. Philos. Trans. R. Soc. Lond. B Biol. Sci. 360, 1001–1013.

Biswal, B., Yetkin, F.Z., Haughton, V.M., Hyde, J.S., 1995. Functional connectivity in the motor cortex of resting human brain using echo-planar MRI. Magn. Reson. Med. 34, 537–541.

Bostan, A.C., Strick, P.L., 2018. The basal ganglia and the cerebellum: nodes in an integrated network. Nat. Rev. Neurosci. 19, 338–350.

Brady Jr., R.O., Gonsalvez, I., Lee, I., Ongur, D., Seidman, L.J., Schmahmann, J.D., Eack, S.M., Keshavan, M.S., Pascual-Leone, A., Halko, M.A., 2019. Cerebellar-Prefrontal Network Connectivity and Negative Symptoms in Schizophrenia. Am. J. Psychiatry 176, 512–520.

Buckner, R.L., 2013. The cerebellum and cognitive function: 25 years of insight from anatomy and neuroimaging. Neuron 80, 807–815.

Buckner, R.L., Sepulcre, J., Talukdar, T., Krienen, F.M., Liu, H., Hedden, T., Andrews-Hanna, J.R., Sperling, R.A., Johnson, K.A., 2009. Cortical hubs revealed by intrinsic functional connectivity: mapping, assessment of stability, and relation to Alzheimer's disease. J. Neurosci. 29, 1860–1873.

Bullmore, E.T., Frangou, S., Murray, R.M., 1997. The dysplastic net hypothesis: an integration of developmental and dysconnectivity theories of schizophrenia. Schizophr. Res. 28, 143–156.

Chang, C.-C., Lin, C.-J., 2011. LIBSVM: A library for support vector machines. ACM Trans. Intell. Syst. Technol. 2, 1–27.

Chang, X., Xi, Y.B., Cui, L.B., Wang, H.N., Sun, J.B., Zhu, Y.Q., Huang, P., Collin, G., Liu, K., Xi, M., Qi, S., Tan, Q.R., Miao, D.M., Yin, H., 2015. Distinct inter-hemispheric dysconnectivity in schizophrenia patients with and without auditory verbal hallucinations. Sci. Rep. 5, 11218.

Chen, Y.L., Tu, P.C., Lee, Y.C., Chen, Y.S., Li, C.T., Su, T.P., 2013. Resting-state fMRI mapping of cerebellar functional dysconnections involving multiple large-scale networks in patients with schizophrenia. Schizophr. Res. 149, 26–34.

Dai, Z., Yan, C., Li, K., Wang, Z., Wang, J., Cao, M., Lin, Q., Shu, N., Xia, M., Bi, Y., He, Y., 2015. Identifying and mapping connectivity patterns of brain network hubs in Alzheimer's Disease. Cereb. Cortex 25, 3723–3742.

Dandash, O., Fornito, A., Lee, J., Keefe, R.S., Chee, M.W., Adcock, R.A., Pantelis, C., Wood, S.J., Harrison, B.J., 2014. Altered striatal functional connectivity in subjects with an at-risk mental state for psychosis. Schizophr. Bull. 40, 904–913.

Duan, M., Chen, X., He, H., Jiang, Y., Jiang, S., Xie, Q., Lai, Y., Luo, C., Yao, D., 2015. Altered basal ganglia network integration in schizophrenia. Front. Hum. Neurosci. 9, 561.

M.B. First L., S.R., Miriam, G., B., W.J., Structured clinical interview for DSM-IV-TR Axis I Disorders, Research Version 2002 Non-patient Edition New York State Psychiatric Institute, New York.

Fornito, A., Harrison, B.J., Goodby, E., Dean, A., Ooi, C., Nathan, P.J., Lennox, B.R., Jones, P.B., Suckling, J., Bullmore, E.T., 2013. Functional dysconnectivity of corticostriatal circuitry as a risk phenotype for psychosis. JAMA Psychiatry 70, 1143–1151.

Friston, K.J., 1998. The disconnection hypothesis. Schizophr. Res. 30, 115–125.

Friston, K., Brown, H.R., Siemerkus, J., Stephan, K.E., 2016. The dysconnection hypothesis (2016). Schizophr. Res. 176, 83–94.

Giraldo-Chica, M., Woodward, N.D., 2017. Review of thalamocortical resting-state fMRI studies in schizophrenia. Schizophr. Res. 180, 58–63.

Greene, D.J., Marek, S., Gordon, E.M., Siegel, J.S., Gratton, C., Laumann, T.O., Gilmore, A.W., Berg, J.J., Nguyen, A.L., Dierker, D., Van, A.N., Ortega, M., Newbold, D.J., Hampton, J.M., Nielsen, A.N., McDermott, K.B., Roland, J.L., Norris, S.A., Nelson, S.M., Snyder, A.Z., Schlaggar, B.L., Petersen, S.E., Dosenbach, N.U.F., 2020. Integrative and network-specific connectivity of the basal ganglia and thalamus defined in individuals. Neuron 105 (742–758), e746.

Greicius, M., 2008. Resting-state functional connectivity in neuropsychiatric disorders. Curr. Opin. Neurol. 21, 424–430.

Greicius, M.D., Krasnow, B., Reiss, A.L., Menon, V., 2003. Functional connectivity in the resting brain: a network analysis of the default mode hypothesis. Proc Natl Acad Sci U S A 100, 253–258.

Greicius, M.D., Srivastava, G., Reiss, A.L., Menon, V., 2004. Default-mode network activity distinguishes Alzheimer's disease from healthy aging: evidence from functional MRI. Proc Natl Acad Sci U S A 101, 4637–4642.

Guimera, R., Nunes Amaral, L.A., 2005. Functional cartography of complex metabolic networks. Nature 433, 895–900.

Habas, C., Kamdar, N., Nguyen, D., Prater, K., Beckmann, C.F., Menon, V., Greicius, M. D., 2009. Distinct cerebellar contributions to intrinsic connectivity networks. J. Neurosci. 29, 8586–8594.

Hall, H., Sedvall, G., Magnusson, O., Kopp, J., Halldin, C., Farde, L., 1994. Distribution of D1- and D2-dopamine receptors, and dopamine and its metabolites in the human brain. Neuropsychopharmacology 11, 245–256.

Hummer, T.A., Yung, M.G., Goni, J., Conroy, S.K., Francis, M.M., Mehdiyoun, N.F., Breier, A., 2020. Functional network connectivity in early-stage schizophrenia. Schizophr. Res. 218, 107–115.

Inada, T., Inagaki, A., 2015. Psychotropic dose equivalence in Japan. Psychiatry Clin. Neurosci. 69, 440–447.

Jao, T., Vertes, P.E., Alexander-Bloch, A.F., Tang, I.N., Yu, Y.C., Chen, J.H., Bullmore, E. T., 2013. Volitional eyes opening perturbs brain dynamics and functional connectivity regardless of light input. Neuroimage 69, 21–34.

Javitt, D.C., 2009. Sensory processing in schizophrenia: neither simple nor intact. Schizophr. Bull. 35, 1059–1064.

Kawabata, K., Watanabe, H., Hara, K., Bagarinao, E., Yoneyama, N., Ogura, A., Imai, K., Masuda, M., Yokoi, T., Ohdake, R., Tanaka, Y., Tsuboi, T., Nakamura, T., Hirayama, M., Ito, M., Atsuta, N., Maesawa, S., Naganawa, S., Katsuno, M., Sobue, G., 2018. Distinct manifestation of cognitive deficits associate with different resting-state network disruptions in non-demented patients with Parkinson's disease. J. Neurol. 265, 688–700.

Kawabata, K., Bagarinao, E., Watanabe, H., Maesawa, S., Mori, D., Hara, K., Ohdake, R., Masuda, M., Ogura, A., Kato, T., Koyama, S., Katsuno, M., Wakabayashi, T., Kuzuya, M., Hoshiyama, M., Isoda, H., Naganawa, S., Ozaki, N., Sobue, G., 2021. Bridging large-scale cortical networks: Integrative and function-specific hubs in the thalamus. iScience 24, 103106.

Kawabata, K., Bagarinao, E., Watanabe, H., Maesawa, S., Mori, D., Hara, K., Ohdake, R., Masuda, M., Ogura, A., Kato, T., Koyama, S., Katsuno, M., Wakabayashi, T., Kuzuya, M., Hoshiyama, M., Isoda, H., Naganawa, S., Ozaki, N., Sobue, G., 2022. Functional connector hubs in the cerebellum. Neuroimage 257, 119263.

Kay, S.R., Fiszbein, A., Opler, L.A., 1987. The positive and negative syndrome scale (PANSS) for schizophrenia. Schizophr. Bull. 13, 261–276.

Kogata, T., Iidaka, T., 2018. A review of impaired visual processing and the daily visual world in patients with schizophrenia. Nagoya J. Med. Sci. 80, 317–328.

Koshiyama, D., Fukunaga, M., Okada, N., Yamashita, F., Yamamori, H., Yasuda, Y., Fujimoto, M., Ohi, K., Fujino, H., Watanabe, Y., Kasai, K., Hashimoto, R., 2018a. Role of subcortical structures on cognitive and social function in schizophrenia. Sci. Rep. 8, 1183.

Koshiyama, D., Fukunaga, M., Okada, N., Yamashita, F., Yamamori, H., Yasuda, Y., Fujimoto, M., Ohi, K., Fujino, H., Watanabe, Y., Kasai, K., Hashimoto, R., 2018b. Subcortical association with memory performance in schizophrenia: a structural magnetic resonance imaging study. Transl. Psychiatry 8, 20.

Li, M., Becker, B., Zheng, J., Zhang, Y., Chen, H., Liao, W., Duan, X., Liu, H., Zhao, J., Chen, H., 2019. Dysregulated maturation of the functional connectome in antipsychotic-naive, first-episode patients with adolescent-onset schizophrenia. Schizophr. Bull. 45, 689–697.

Liu, Y., Liang, M., Zhou, Y., He, Y., Hao, Y., Song, M., Yu, C., Liu, H., Liu, Z., Jiang, T., 2008. Disrupted small-world networks in schizophrenia. Brain 131, 945–961.

Liu, X., Yang, H., Becker, B., Huang, X., Luo, C., Meng, C., Biswal, B., 2021. Disentangling age- and disease-related alterations in schizophrenia brain network using structural

equation modeling: A graph theoretical study based on minimum spanning tree. Hum. Brain Mapp. 42, 3023–3041.
Lynall, M.E., Bassett, D.S., Kerwin, R., McKenna, P.J., Kitzbichler, M., Muller, U., Bullmore, E., 2010. Functional connectivity and brain networks in schizophrenia. J. Neurosci. 30, 9477–9487.
Macpherson, T., Hikida, T., 2019. Role of basal ganglia neurocircuitry in the pathology of psychiatric disorders. Psychiatry Clin. Neurosci. 73, 289–301.
J.K. Mai . P.G., The Human Nervous System 3rd ed. 2012 Academic Press (Elsevier) Massachusetts.
Martino, M., Magioncalda, P., Yu, H., Li, X., Wang, Q., Meng, Y., Deng, W., Li, Y., Li, M., Ma, X., Lane, T., Duncan, N.W., Northoff, G., Li, T., 2018. Abnormal resting-state connectivity in a substantia nigra-related striato-thalamo-cortical network in a large sample of first-episode drug-naive patients with schizophrenia. Schizophr. Bull. 44, 419–431.
Matsuoka, K., Uno, M., Kasai, K., Koyama, K., Kim, Y., 2006. Estimation of premorbid IQ in individuals with Alzheimer's disease using Japanese ideographic script (Kanji) compound words: Japanese version of National Adult Reading Test. Psychiatry Clin. Neurosci. 60, 332–339.
Menon, V., 2011. Large-scale brain networks and psychopathology: a unifying triple network model. Trends Cogn Sci 15, 483–506.
Milardi, D., Quartarone, A., Bramanti, A., Anastasi, G., Bertino, S., Basile, G.A., Buonasera, P., Pilone, G., Celeste, G., Rizzo, G., Bruschetta, D., Cacciola, A., 2019. The cortico-basal ganglia-cerebellar network: past, present and future perspectives. Front. Syst. Neurosci. 13, 61.
Mugler 3rd, J.P., Brookeman, J.R., 1990. Three-dimensional magnetization-prepared rapid gradient-echo imaging (3D MP RAGE). Magn. Reson. Med. 15, 152–157.
Okada, N., Fukunaga, M., Yamashita, F., Koshiyama, D., Yamamori, H., Ohi, K., Yasuda, Y., Fujimoto, M., Watanabe, Y., Yahata, N., Nemoto, K., Hibar, D.P., van Erp, T.G., Fujino, H., Isobe, M., Isomura, S., Natsubori, T., Narita, H., Hashimoto, N., Miyata, J., Koike, S., Takahashi, T., Yamasue, H., Matsuo, K., Onitsuka, T., Iidaka, T., Kawasaki, Y., Yoshimura, R., Watanabe, Y., Suzuki, M., Turner, J.A., Takeda, M., Thompson, P.M., Ozaki, N., Kasai, K., Hashimoto, R., 2016. Abnormal asymmetries in subcortical brain volume in schizophrenia. Mol. Psychiatry 21, 1460–1466.
Okada, N., Yahata, N., Koshiyama, D., Morita, K., Sawada, K., Kanata, S., Fujikawa, S., Sugimoto, N., Toriyama, R., Masaoka, M., Koike, S., Araki, T., Kano, Y., Endo, K., Yamasaki, S., Ando, S., Nishida, A., Hiraiwa-Hasegawa, M., Kasai, K., 2018. Abnormal asymmetries in subcortical brain volume in early adolescents with subclinical psychotic experiences. Transl. Psychiatry 8, 254.
Oldfield, R.C., 1971. The assessment and analysis of handedness: the Edinburgh inventory. Neuropsychologia 9, 97–113.
Owen, M.J., Sawa, A., Mortensen, P.B., 2016. Schizophrenia. Lancet 388, 86–97.
Power, J.D., Mitra, A., Laumann, T.O., Snyder, A.Z., Schlaggar, B.L., Petersen, S.E., 2014. Methods to detect, characterize, and remove motion artifact in resting state fMRI. Neuroimage 84, 320–341.
Power, J.D., Schlaggar, B.L., Petersen, S.E., 2015. Recent progress and outstanding issues in motion correction in resting state fMRI. Neuroimage 105, 536–551.
Quide, Y., Morris, R.W., Shepherd, A.M., Rowland, J.E., Green, M.J., 2013. Task-related fronto-striatal functional connectivity during working memory performance in schizophrenia. Schizophr. Res. 150, 468–475.
Rubinov, M., Bullmore, E., 2013. Schizophrenia and abnormal brain network hubs. Dialogues Clin Neurosci 15, 339–349.
Rubinov, M., Sporns, O., 2010. Complex network measures of brain connectivity: uses and interpretations. Neuroimage 52, 1059–1069.
Sarpal, D.K., Robinson, D.G., Lencz, T., Argyelan, M., Ikuta, T., Karlsgodt, K., Gallego, J. A., Kane, J.M., Szeszko, P.R., Malhotra, A.K., 2015. Antipsychotic treatment and functional connectivity of the striatum in first-episode schizophrenia. JAMA Psychiatry 72, 5–13.
Sasabayashi, D., Takayanagi, Y., Takahashi, T., Katagiri, N., Sakuma, A., Obara, C., Katsura, M., Okada, N., Koike, S., Yamasue, H., Nakamura, M., Furuichi, A., Kido, M., Nishikawa, Y., Noguchi, K., Matsumoto, K., Mizuno, M., Kasai, K., Suzuki, M., 2020. Subcortical brain volume abnormalities in individuals with an at-risk mental state. Schizophr. Bull. 46, 834–845.
Seeley, W.W., Menon, V., Schatzberg, A.F., Keller, J., Glover, G.H., Kenna, H., Reiss, A.L., Greicius, M.D., 2007. Dissociable intrinsic connectivity networks for salience processing and executive control. J. Neurosci. 27, 2349–2356.
Sendi, M.S.E., Pearlson, G.D., Mathalon, D.H., Ford, J.M., Preda, A., van Erp, T.G.M., Calhoun, V.D., 2021. Multiple overlapping dynamic patterns of the visual sensory network in schizophrenia. Schizophr. Res. 228, 103–111.
Sherman, S.M., 2016. Thalamus plays a central role in ongoing cortical functioning. Nat. Neurosci. 19, 533–541.
Shirer, W.R., Ryali, S., Rykhlevskaia, E., Menon, V., Greicius, M.D., 2012. Decoding subject-driven cognitive states with whole-brain connectivity patterns. Cereb. Cortex 22, 158–165.
Sporns, O., Honey, C.J., Kotter, R., 2007. Identification and classification of hubs in brain networks. PLoS ONE 2, e1049.
Stoodley, C.J., Schmahmann, J.D., 2010. Evidence for topographic organization in the cerebellum of motor control versus cognitive and affective processing. Cortex 46, 831–844.
Sui, J., Pearlson, G.D., Du, Y., Yu, Q., Jones, T.R., Chen, J., Jiang, T., Bustillo, J., Calhoun, V.D., 2015. In search of multimodal neuroimaging biomarkers of cognitive deficits in schizophrenia. Biol. Psychiatry 78, 794–804.
van den Heuvel, M.P., Kahn, R.S., 2011. Abnormal brain wiring as a pathogenetic mechanism in schizophrenia. Biol. Psychiatry 70, 1107–1108.
van den Heuvel, M.P., Sporns, O., 2013. Network hubs in the human brain. Trends Cogn Sci 17, 683–696.
van den Heuvel, M.P., Sporns, O., Collin, G., Scheewe, T., Mandl, R.C., Cahn, W., Goni, J., Hulshoff Pol, H.E., Kahn, R.S., 2013. Abnormal rich club organization and functional brain dynamics in schizophrenia. JAMA Psychiatry 70, 783–792.
Wang, L., Metzak, P.D., Honer, W.G., Woodward, T.S., 2010. Impaired efficiency of functional networks underlying episodic memory-for-context in schizophrenia. J. Neurosci. 30, 13171–13179.
Wang, L., Zou, F., Shao, Y., Ye, E., Jin, X., Tan, S., Hu, D., Yang, Z., 2014. Disruptive changes of cerebellar functional connectivity with the default mode network in schizophrenia. Schizophr. Res. 160, 67–72.
Yamamoto, M., Kushima, I., Suzuki, R., Branko, A., Kawano, N., Inada, T., Iidaka, T., Ozaki, N., 2018. Aberrant functional connectivity between the thalamus and visual cortex is related to attentional impairment in schizophrenia. Psychiatry Res Neuroimaging 278, 35–41.
Yokoi, T., Watanabe, H., Yamaguchi, H., Bagarinao, E., Masuda, M., Imai, K., Ogura, A., Ohdake, R., Kawabata, K., Hara, K., Riku, Y., Ishigaki, S., Katsuno, M., Miyao, S., Kato, K., Naganawa, S., Harada, R., Okamura, N., Yanai, K., Yoshida, M., Sobue, G., 2018. Involvement of the Precuneus/Posterior Cingulate Cortex Is Significant for the Development of Alzheimer's Disease: A PET (THK5351, PiB) and Resting fMRI Study. Front. Aging Neurosci. 10, 304.
Yoneyama, N., Watanabe, H., Kawabata, K., Bagarinao, E., Hara, K., Tsuboi, T., Tanaka, Y., Ohdake, R., Imai, K., Masuda, M., Hattori, T., Ito, M., Atsuta, N., Nakamura, T., Hirayama, M., Maesawa, S., Katsuno, M., Sobue, G., 2018. Severe hyposmia and aberrant functional connectivity in cognitively normal Parkinson's disease. PLoS ONE 13, e0190072.
Zhou, Y., Liang, M., Jiang, T., Tian, L., Liu, Y., Liu, Z., Liu, H., Kuang, F., 2007. Functional dysconnectivity of the dorsolateral prefrontal cortex in first-episode schizophrenia using resting-state fMRI. Neurosci. Lett. 417, 297–302.